

2-1

"Made available under NASA sponsorship
in the interest of early and wide dis-
semination of Earth Resources Survey
Program information and without liability
for any use made thereof."

E7.3 10369
CR 131010

TYPE II PROGRESS REPORT
For Period Ending
2/16/73

A Study to Explore the Use of Orbital Remote Sensing
to Determine Native Arid Plant Distribution
MMC #250, GSFC # UN 613

Principal Investigators: William G. McGinnies and
Edward F. Haase

This progress report was compiled by H. Brad Musick

Office of Arid Lands Studies, University of Arizona

Original photography may be purchased from:
EROS Data Center
10th and Dakota Avenue
Sioux Falls, SD 57198

(E73-10369) A STUDY TO EXPLORE THE USE OF ORBITAL REMOTE SENSING TO DETERMINE NATIVE ARID PLANT DISTRIBUTION Progress Report, period ending 16 Feb. (Arizona Univ., Tucson.) 28 p HC \$3.50 CSCL 08F	N73-19365 Unclas G3/13 00369
--	--

ACCOMPLISHMENTS:

Accomplishments during the first six months of the investigation fall into three general categories. In the Avra Valley area, about 15 miles west of Tucson, we are exploring the use of low platform 35mm color and color IR photography to aid in the interpretation of ERTS-1 MSS imagery. We are exploring the use of light table analysis, the I2S multispectral color additive viewer, and a Spatial Data Systems video display density analyzer to construct a pre-typed image of the Tucson area from ERTS imagery. We have also developed the theory of a method for obtaining reflectivity measurements and spectral signatures of areas from a combination of ERTS-1 MSS data and certain ground truth data from calibration areas.

Avra Valley Study Area

We have established nine study sites in and around the Avra Valley west of Tucson, Arizona. These sites are representative of most of the major plant communities which occur in the area, such as creosote bush (Larrea divaricata) desert, palo verde (Cercidium spp.)-saguaro (Carnegiea gigantea) desert, desert grassland, and other communities. The vegetational composition at each site has been estimated, and observations on phenological developments are being made periodically. Matching 35mm color and color IR photographs of the areas were taken from a low platform at two times, in late November 1972 and in early February 1973. Some color and color IR photography and observations have been made in other areas of the valley.

The Avra Valley area has been studied on the following ERTS MSS images:

(22 Aug. 1971) 1030-17271 all bands (70mm and 9.5 inch bulk black and white transparencies)

(2 Nov. 1971) 1102-17280 all bands (70mm and 9.5 inch bulk black and white transparencies)

(2 Nov. 1971) 1102-17274 all bands (70mm and 9.5 inch bulk black and white transparencies)

and on high-altitude aircraft photography (ERAP Mission 101). The ERTS imagery was analyzed on a light table with hand lens, on a video display density analyzer, and on a multispectral additive color viewer.

Results of analysis of Avra Valley imagery and correlation with ground truth data

1. High-altitude aircraft photography was useful for preliminary reconnaissance of the area, and for picking large homogeneous areas for the study sites.

2. For areas of this size (one to five square miles), 9.5 inch MSS imagery is preferred over 70mm imagery for analysis on the light table and the density analyzer because of its larger scale.

3. On these images, differences in spectral signature between most sites appear to be slight. This may be partly the result of the relatively low vegetative cover of these sites and the low infrared reflectivity of many desert plants.

4. Dense mesquite tree stands with crown cover approaching 100% are easily recognized on MSS imagery by their low reflectivity in the visible bands and their characteristic occurrence on the floodplains of the larger drainageways.

5. The desert grassland site and the mesquite-burroweed site differ in overall reflectivity on these ERTS images. The bajada and associated pediment of the Sierrita Mountains can be differentiated on the ERTS imagery into two zones which differ in reflectivity: an upper zone, which is darker in all bands, and a lower zone which is lighter in all bands. (Figure 1)

The contact between the two zones is relatively sharp, except for some very narrow extensions of the darker zone down into the lighter zone. Our desert grassland study site is in the main body of the darker upper zone, and our mesquite-burroweed study site is in the lighter lower zone. The two zones can also be recognized on high altitude aircraft support photography. (Figure 2)

Examination of this photography revealed that our mesquite-burroweed site is in a small area of intermediate reflectivity (between the lightest part of light zone and a darker "island" in the light zone). An area of lower reflectivity in the light zone, and a very light adjacent area were picked out on the aircraft photography for ground checking. Ground checking indicated that the light area is severely sheet-eroded, with only a few scattered mesquites and much bare sandy soil. (Figures 3 and 4)

Reproduced from
best available copy.

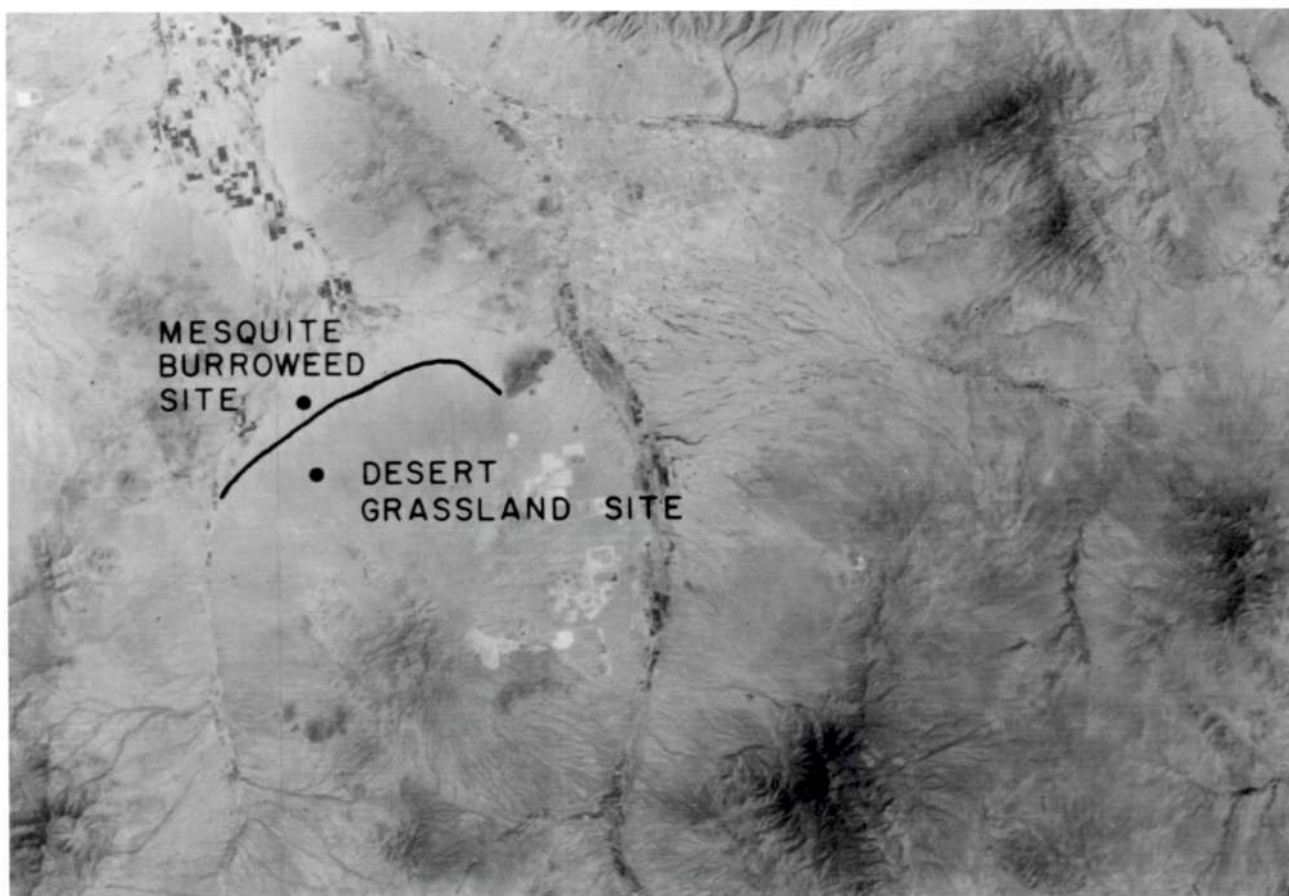


Figure 1. Portion of ERTS image(22 Aug. 72) E-1030-17271-5 showing the locations of the Sierrita Mtn. bajada study sites. The line between the two sites indicates the approximate boundary between the eroded lower bajada and the relatively uneroded upper bajada.

Reproduced from
best available copy.

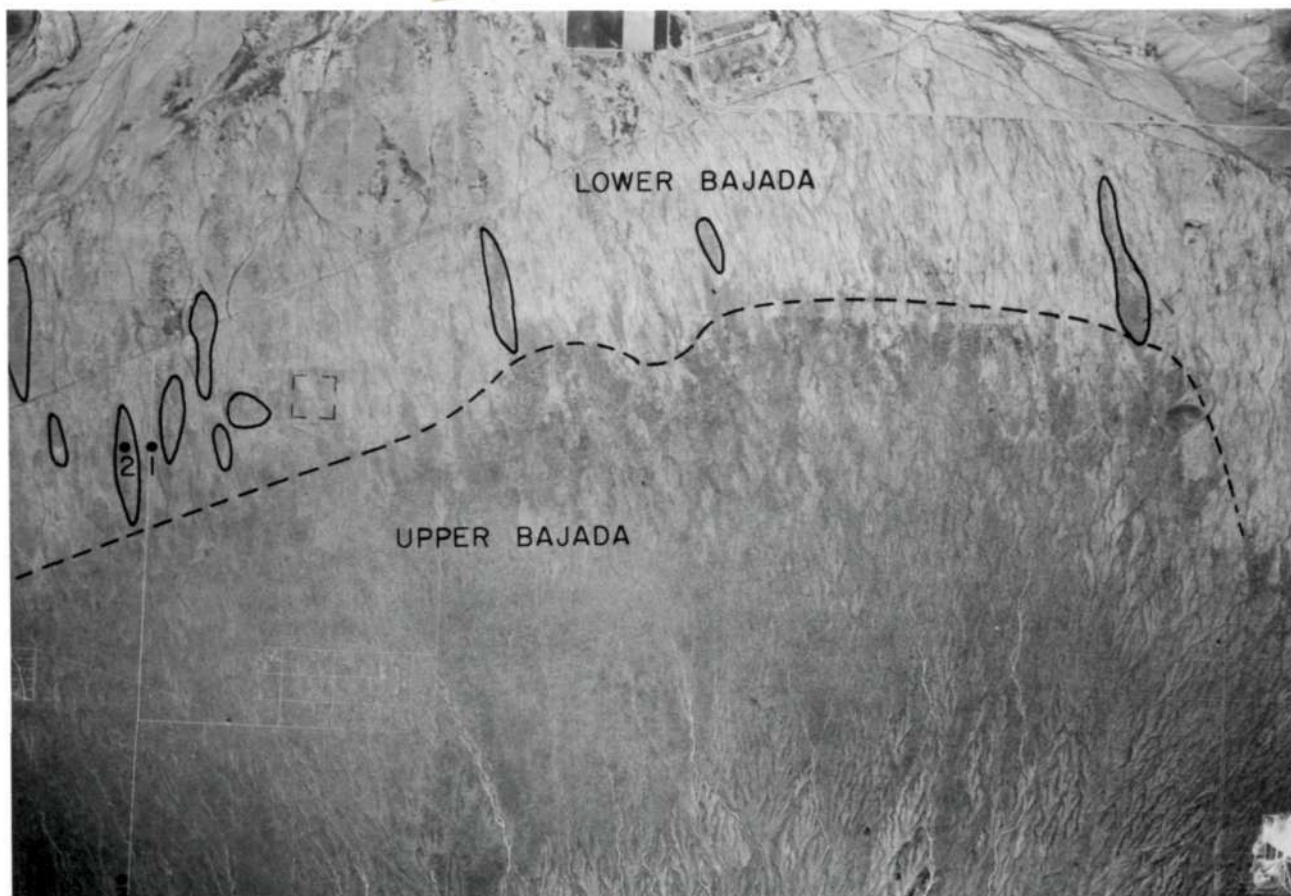


Figure 2. Frame 4751 of color infrared photography of EOAP Mission 101 (10 Aug. 69) showing the northern Sierrita Mtn. bajada. Line is the approximate boundary between the lower and upper parts of the bajada. Some of the darker areas on the lower bajada are outlined. No. 1 is the location of Figures 3 and 4; No. 2 is the location of Figures 5 and 6. No. 3 is the location of Figure 7.

Reproduced from
best available copy.



Figure 3. Vertical color infrared photograph from a low platform on the eroded lower bajada (Location 1 of Figure 2) 8 Dec. 72.

Reproduced from
best available copy.



Figure 4. High oblique color infrared photograph from a low platform on the eroded lower bajada (view to the north at Location 1 of Figure 2) 8 Dec. 72.

The darker island in the light zone has scattered mesquite with a ground cover of burroweed (Haplopappus tenuisecta), snakeweed (Gutierrezia lucida), small perennial grasses and annual grass litter. (Figures 5 and 6)

The dark desert grassland site, farther up the bajada, has scattered mesquite and palo verde, several species of shrubs and subshrubs, some large perennial grasses, and litter largely of annual grasses. (Figure 7)

This ground truth information suggests that the darker upper bajada and the dark islands on the lighter lower bajada are darker because they have a lesser amount of exposed light-colored soil. Although the species compositions of the dark islands and the upper bajada are different, their respective spectral signatures do not appear to differ greatly. However, more refined techniques for determining spectral signature may reveal a difference. Comparisons of these two dark areas has been difficult because of the small size of the dark islands on the ERTS imagery.

The contrast between these light and dark areas is least in MSS band 4 on the 22 Aug. imagery. Contrast between the light lower bajada and the dark islands is about the same in bands 5, 6, and 7. Contrast between the upper bajada and the lower bajada is greatest in band 5. Reduced contrast in the IR bands is probably due to IR reflection by the annual and perennial grasses which were actively growing on the upper bajada at this time.

6. On ERTS MSS images of 22 Aug. 1972 and 2 Nov. 1972, the palo verde-saguaro site on alluvium derived from rhyolite is slightly less reflective than the palo verde-saguaro site on alluvium derived from granite. (Figure 8)

The two sites differ somewhat in vegetative composition and soil surface color. 35mm color IR photography from a low platform indicates that the rhyolite alluvium soil surface is darker. (Figures 9 and 10)

Reproduced from
best available copy.



Figure 5. Vertical color infrared photograph from a low platform on one of the darker areas of the lower bajada (Location 2 of Figure 2) 8 Dec. 72.



Figure 6. High oblique color infrared photograph from a low platform on one of the darker areas of the lower bajada (view to the north at Location 2 of Figure 2) 8 Dec. 72.

Reproduced from
best available copy.



Figure 7. Low oblique color infrared photograph from a low platform on the upper bajada (view to the north at Location 3 of Figure 2, desert grassland site) 20 Nov. 72.

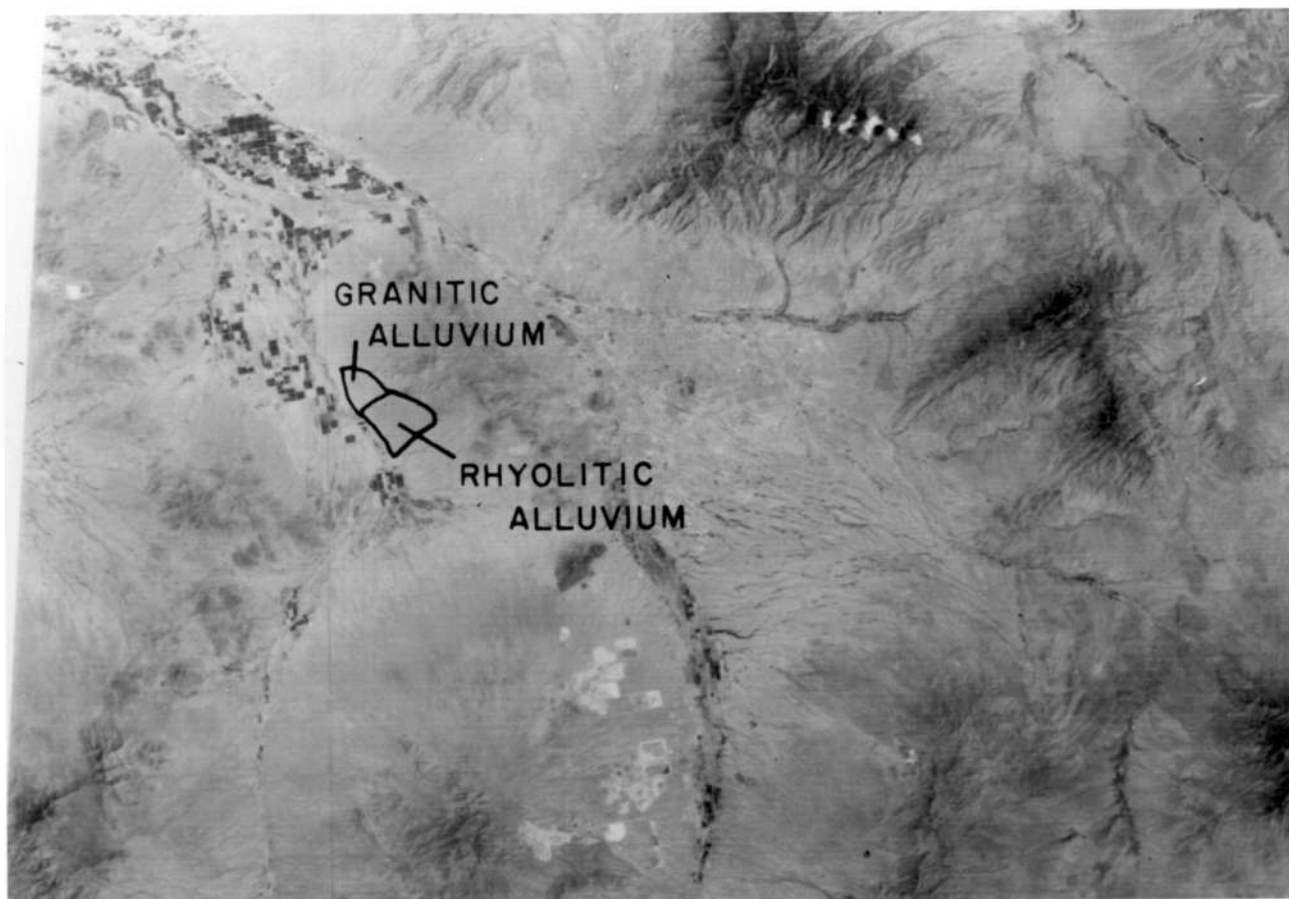


Figure 8. Portion of ERTS image 22 Aug. 72, E-1030-17271-7 showing the locations of the rhyolitic alluvium area and part of the granitic alluvium area on the western bajada of the Tucson Mountains.

Reproduced from
best available copy.



Figure 9. Low oblique color infrared photograph from a low platform on the granitic alluvium area of Figure 8, view to the northeast (21 Nov. 72). Small shrubs are Franseria deltoidea.

Reproduced from
best available copy.

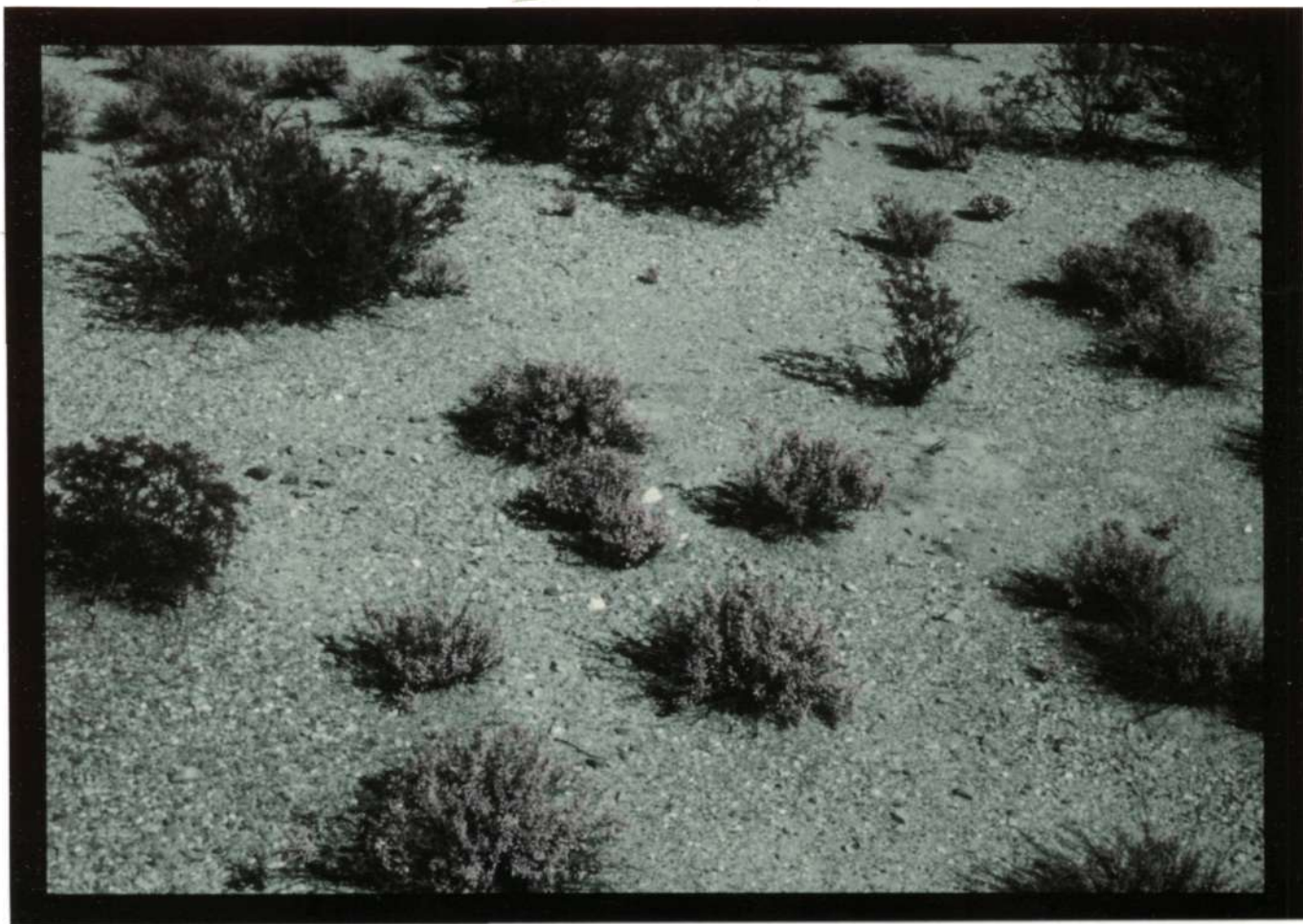


Figure 10. Low oblique color infrared photograph from a low platform on the rhyolitic alluvium area of Figure 8, view to the northeast (21 Nov. 72) Small shrubs are Franseria deltoidea.

Reflectivity of the rhyolite rock fragments on the surface is lower in the green and IR wavelengths than in the red wavelengths. The reflectivity of the granite alluvium is relatively uniform and high. On the 22 Aug. 1972 imagery, the contrast between these sites is least in band 5 (red) and greater in band 7 (IR). This is what would be expected if the observed soil surface color difference was responsible for the contrast between the areas. Evaluation of the role of vegetation in the color difference would seem to require imagery which gives a vertical view of the small trees but is of a sufficiently large scale that individual trees and shrubs could be identified.

Pre-typed image of Tucson area

To supplement the detailed analysis of the Avra Valley sites, we are also evaluating a mapping approach to the determination of the distribution of plant communities. In this approach we will pre-type an area using ERTS imagery. The type lines will be redefined using high-altitude photography, geologic maps, ground truth data and other information.

Pre-typing of an image which includes the Tucson vicinity has been done on the basis of two criteria: (a) landform, and (b) brightness in band 5 (red). Pre-typing was done on a 9.5 inch black and white bulk transparency, since the 70mm format is too small for the methods employed. Using the light table and hand magnifier, the area was differentiated into two landform types: mountains, and non-mountainous terrain (bajadas, plains, hills and valleys). The video display densitometer was used to differentiate the area into four levels of gray on the red band image, and the boundaries of these gray levels were marked on a transparent overlay. Then the two overlays were combined, resulting in a type map which identifies each area by landform type and relative radiance in the red band. (Figure 11)

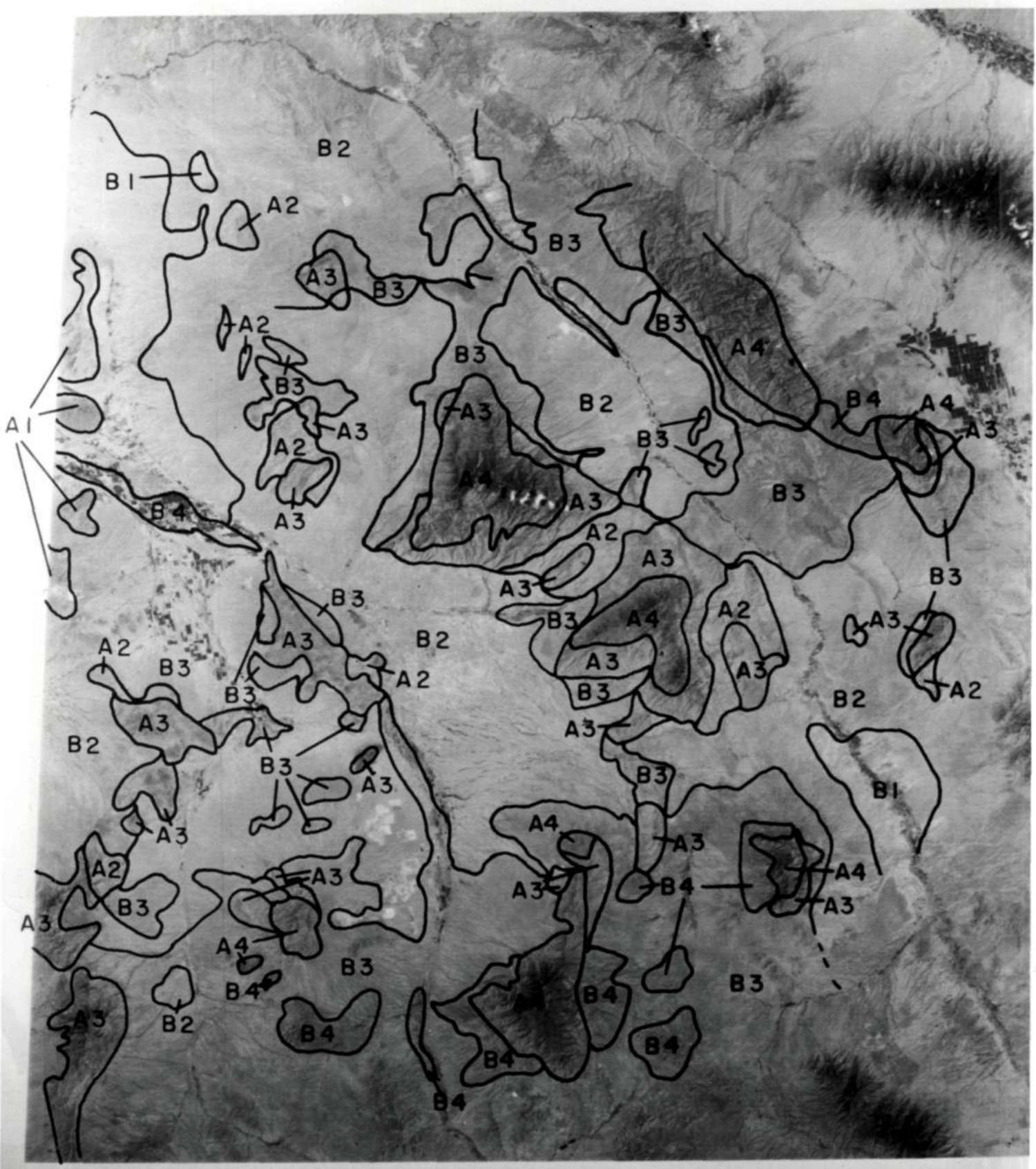
Information from geologic maps, high-altitude photography and other sources can be used to predict the vegetation types of the mapped areas. Ground truth data can be used to determine the accuracy of the resulting map. Other methods of deriving type maps from ERTS data may be explored and compared with the above method.

Figure 11. ERTS image 22 Aug. 72, E-1030-17271-5 pre-typed by terrain class and brightness in band 5 (red).

Key to symbols:

- | | |
|--------------------------------|---|
| A - mountainous terrain | 1 - lightest in band 5 |
| B - bajadas, plains, low hills | 2,3 - intermediate brightness in band 5 |
| | 4 - darkest in band 5 |

Reproduced from
best available copy.



Spectral signature determinations from ERTS-1 MSS data

If ground truth data on the correlations of vegetation characteristics with spectral signature are obtained, and if spectral signatures of the same areas can be determined from ERTS multispectral data, then we can hypothesize on the vegetational characteristics of areas where no ground truth data are available. Accurate determination of the reflectivity of areas directly from the ERTS data is impossible without taking atmospheric effects into account.

A model which describes the relationship between light incident on the scene, atmospheric effects, scene characteristics, and the resulting scene radiance as sensed by the multispectral sensor is described below. This model was presented to us by Dr. Philip N. Slater of the University of Arizona Optical Sciences Center. Dr. Larry K. Lepley, Coordinator of the Arizona Regional Ecological Test Site, also contributed many helpful ideas.

The radiance of an area of spatially uniform reflectivity as sensed by the spacecraft sensor (I_{sensor}) is given by the following equation:

$$I_{\text{sensor}} = (I_{\text{sun}} + I_{\text{sky}}) \rho \tau + I_{\text{us}}$$

where:

- I_{sun} = direct solar radiation incident on the area
- I_{sky} = diffuse sky radiation incident on the area
- ρ = reflectivity of the area
- τ = transmissivity of the atmosphere along the path from the scene to the spacecraft
- I_{us} = radiant energy scattered upwards by the atmosphere over the area

All of these terms are wavelength-dependent but the subscript λ has been omitted for clarity.

H. B. Musick from our investigation team has developed the theory of a method for determining the reflectivity of an area from ERTS data which requires a limited amount of ground truth data if certain assumptions are made. This theory is derived from the model presented by Dr. P. N. Slater which is described above.

Suppose that radiance values (I_A , I_B , I_X) are available for three areas, A, B, and X, from spacecraft data of a given date. A and B are calibration areas for which the reflectivities (ρ_A and ρ_B , where $\rho_A \neq \rho_B$) are known from ground truth measurements. The problem is to determine the reflectivity of area X (ρ_X), for which no ground truth spectral signature data are available. If certain assumptions can be made, the reflectivity of area X can be expressed in terms of I_A , I_B , ρ_A and ρ_B , as shown below.

Using the basic equation given above which describes the relationship between the energy incident on the sensor and atmospheric and reflectivity effects, solve for ρ_A and ρ_B :

$$I_A = (I_{\text{sun}} + I_{\text{sky}}) \rho_A \tau + I_{\text{us}}$$

$$(I_{\text{sun}} + I_{\text{sky}}) \rho_A \tau = I_A - I_{\text{us}}$$

$$\rho_A = \frac{I_A - I_{\text{us}}}{(I_{\text{sun}} + I_{\text{sky}}) \tau}$$

Similarly,

$$\rho_B = \frac{I_B - I_{\text{us}}}{(I_{\text{sun}} + I_{\text{sky}}) \tau}$$

Assuming that $[(I_{\text{sun}} + I_{\text{sky}}) \tau]$ and I_{us} are the same for both sites at the time of the overflight, solve for $\frac{\rho_A}{\rho_B}$:

$$\frac{\rho_A}{\rho_B} = \frac{I_A - I_{us}}{(I_{sun} + I_{sky}) \tau} \cdot \frac{(I_{sun} + I_{sky}) \tau}{I_B - I_{us}}$$

$$\frac{\rho_A}{\rho_B} = \frac{I_A - I_{us}}{I_B - I_{us}}$$

Solve this equation for I_{us} in terms of I_A , I_B , ρ_A , and ρ_B :

$$\rho_A (I_B - I_{us}) = \rho_B (I_A - I_{us})$$

$$\rho_A I_B - \rho_A I_{us} = \rho_B I_A - \rho_B I_{us}$$

$$\rho_B I_{us} - \rho_A I_{us} = \rho_B I_A - \rho_A I_B$$

$$I_{us} (\rho_A - \rho_B) = \rho_B I_A - \rho_A I_B$$

$$I_{us} = \frac{\rho_B I_A - \rho_A I_B}{\rho_A - \rho_B}$$

For a given date and wavelength, we now have a numerical value for I_{us} . We can substitute this value into the original equation for I_A or I_B to obtain a numerical value for the term $[(I_{sun} + I_{sky}) \tau]$:

$$\text{As before, } I_A = (I_{sun} + I_{sky}) \rho_A \tau + I_{us}$$

$$\rho_A = \frac{I_A - I_{us}}{(I_{sun} + I_{sky}) \tau}$$

$$(I_{sun} + I_{sky}) \tau = \frac{I_A - I_{us}}{\rho_A}$$

We now have numerical values for both I_{us} and $[(I_{sun} + I_{sky})\tau]$.

If our area X is near enough to areas A and B that we can assume that the radiation incident on site X and the effects of the atmosphere over area X are essentially the same as for areas A and B, then we can use the numerical values of I_{us} and $[(I_{sun} + I_{sky})\tau]$ and the spacecraft measurement of I_X to determine ρ_X :

$$I_X = (I_{sun} + I_{sky}) \rho_X \tau + I_{us}$$

$$\rho_X = \frac{I_X - I_{us}}{(I_{sun} + I_{sky}) \tau}$$

Since the values of I_{us} and $[(I_{sun} + I_{sky})\tau]$ were determined from ρ_A, ρ_B, I_A and I_B , this equation can also be written in terms of these reflectivity and radiance values and I_X :

Substituting for $(I_{sun} + I_{sky})\tau$:

$$\rho_X = \frac{I_X - I_{us}}{(I_{sun} + I_{sky}) \tau} = \frac{I_X - I_{us}}{\left[\frac{I_A - I_{us}}{\rho_A} \right]}$$

Substituting for I_{us} :

$$= \frac{I_X - \left[\frac{\rho_B I_A - \rho_A I_B}{\rho_B - \rho_A} \right]}{\left[\frac{I_A - \left(\frac{\rho_B I_A - \rho_A I_B}{\rho_B - \rho_A} \right)}{\rho_A} \right]}$$

Simplifying:

$$= \frac{\rho_A \left[I_X - \left(\frac{\rho_B I_A - \rho_A I_B}{\rho_B - \rho_A} \right) \right]}{I_A - \left[\frac{\rho_B I_A - \rho_A I_B}{\rho_B - \rho_A} \right]}$$

$$= \frac{\rho_A \left[\frac{I_X (\rho_B - \rho_A) - \rho_B I_A + \rho_A I_B}{\rho_B - \rho_A} \right]}{\left[\frac{I_A (\rho_B - \rho_A) - \rho_B I_A + \rho_A I_B}{\rho_B - \rho_A} \right]}$$

$$= \frac{\rho_A [I_X (\rho_B - \rho_A) - \rho_B I_A + \rho_A I_B]}{I_A (\rho_B - \rho_A) - \rho_B I_A + \rho_A I_B}$$

This equation can be applied to data of each of the ERTS MSS wavelength bands and the spectral signatures of areas can be expressed in terms of reflectivity ratios. The ratio of infrared reflectivity to red reflectivity would be useful in vegetation studies, since vigorous green foliage reflects strongly in the infrared but weakly in the red. Other surfaces, such as desert sand, have reflectivity ratios approaching unity.

Recall that the assumption was made that I_{us} and $[(I_{sun} + I_{sky}) \tau]$ were the same for areas A, B, and X at the time of the overflight. If some additional assumptions are made, the ground truth data (ρ_A and ρ_B) do not have to be taken at the time of the overflight, but can be taken on another day. This would be a very advantageous situation for investigators such as ourselves who have limited access to the instrument which measures reflectivity. We would not always be able to have the instrument on overflight days, and two instruments might be necessary to obtain reflectivity data for the two calibration areas simultaneously.

The reflectivities of the calibration areas A and B at the time ground truth data are taken must be the same as on overflight day. Repeated reflectivity measurements of possible calibration areas would indicate which areas had stable reflectivity, and what the effects of environmental changes were on reflectivity. From these data it should be possible to pick dates on which the reflectivity of the area would be nearly the same as on the overflight day.

There is also the problem of directional reflectance. For many surfaces, the amount of reflected radiation seen by a sensor depends on its view angle relative to the surface and on the angle of the incident radiation. Therefore, the reflectivities must be measured at some time when the sun's angle of elevation is the same as at overflight time. Of course, the reflected radiation must be measured from the same view angle as that of the spacecraft sensor. This accounts for directional reflectance effects on direct solar radiation, but not for directional reflectance effects on diffuse sky radiation. Even with the same sun angle, variations in atmospheric turbidity will change the distribution of the diffuse radiation over the sky. This effect would be minimized by using ground and spacecraft data for cloudless days only. If this is done, and if the surface is a fairly diffuse reflector, then it is assumed that reflectivity measurements obtained on a day other than that of an ERTS overflight can be applied to the ERTS data without appreciable error.

In summary, we believe that this method of determining spectral properties of natural surfaces from spacecraft data has many advantages if the necessary assumptions can be made. It accounts for the effects of sun angle and atmosphere on the scene radiance at the spacecraft sensor. The method also has certain advantages over the other possible methods of correcting for these effects. Since the reflectivity values are ratios, instrument calibration is not as critical as if absolute radiation measurements were necessary. Only one ground truth parameter (reflectivity) is necessary and this can be obtained from two measurements for each wavelength band: total incoming radiation, and vertically reflected radiation. A very important advantage is that the necessary ground truth data can be collected at times other than the overflight time.

We are currently exploring the feasibility of this method for determining reflectivities of areas from spacecraft data. We may be able to determine reflectivity at ground level with the use of an Exotech ERTS radiometer. Radiance values for the areas would be determined by densitometric correlation with the gray scale on the MSS images.

PROBLEMS

Poor contrast of the lighter desert areas on ERTS MSS imagery continues to hinder the study of these areas. We anticipate a requirement for retrospectively ordered imagery with enhanced contrast in these areas.

SIGNIFICANT RESULTS

We have developed the theory of a method for determining the reflectivities of natural areas from ERTS data. This method requires the following measurements: 1) ground truth reflectivity data from two different calibration areas, 2) radiance data from ERTS MSS imagery for the same two calibration areas, and 3) radiance data from ERTS MSS imagery for the area(s) in which reflectivity is to be determined. The method takes into account sun angle effects and atmospheric effects on the radiance seen by the space sensor. If certain assumptions are made, the ground truth data collection need not be simultaneous with the ERTS overflight. The method allows the calculation of a conversion factor for converting ERTS MSS radiance measurements of a given overflight to reflectivity values. This conversion factor can be used to determine the reflectivity of any area in the general vicinity of the calibration areas which has a relatively similar overlying atmosphere. This method, or some modification of it, may be useful in ERTS investigations which require the determination of spectral signatures of areas from spacecraft data.

Published Articles, Etc.: None

Recommendations: None

Changes in Standing Order Forms: None

ERTS Image Descriptor Forms:

ERTS IMAGE DESCRIPTOR FORM

(See Instructions on Back)

26

DATE 17 Feb. '73PRINCIPAL INVESTIGATOR W.G. McGinniesGSFC UN 613ORGANIZATION Office of Arid Lands Studies, University of Arizona

NDPF USE ONLY

D _____

N _____

ID _____

PRODUCT ID (INCLUDE BAND AND PRODUCT)	FREQUENTLY USED DESCRIPTORS*			DESCRIPTORS
	Bajada	Mountain	Alluvial Plain	
1030-17271 M	X	X	X	Erosion, Alkali Flat,
1102-17280 M	X	X	X	Alluvial Fan, Arroyo,
1102-17274 M	X	X	X	Basin and Range,
				Cropland, Desert, Forest
				Grassland, Metropolitan
				Area, Pediment, Rangeland
				Scrub, Valley

*FOR DESCRIPTORS WHICH WILL OCCUR FREQUENTLY, WRITE THE DESCRIPTOR TERMS IN THESE COLUMN HEADING SPACES NOW AND USE A CHECK (✓) MARK IN THE APPROPRIATE PRODUCT ID LINES. (FOR OTHER DESCRIPTORS, WRITE THE TERM UNDER THE DESCRIPTORS COLUMN).

MAIL TO ERTS USER SERVICES
 CODE 563
 BLDG 23 ROOM E413
 NASA GSFC
 GREENBELT, MD. 20771
 301-982-5406

Data Request Forms:

10/31/72

11/17/72

12/7/72

Other Information:

None